COMMISSIONING PROGRESS OF THE RHIC ELECTRON LENSES*

W. Fischer†, Z. Altinbas, M. Anerella, M. Blaskiewicz, D. Bruno, W.C. Dawson, D.M. Gassner, X. Gu, R.C. Gupta, K. Hamdi, J. Hock, L.T. Hoff, R. Hulsart, A.K. Jain, R. Lambiase, Y. Luo, M. Mapes, A. Marone, R. Michnoff, T.A. Miller, M. Minty, C. Montag, J. Muratore, S. Nemesure, D. Phillips, A.I. Pikin, S.R. Plate, P. Rosas, L. Snydstrup, Y. Tan, C. Theisen, P. Thieberger, J. Tuozzolo, P. Wanderer, S.M. White, W. Zhang; BNL, Upton, New York, USA

Abstract

In polarized proton operation, the RHIC performance is limited by the head-on beam-beam effect. To overcome these limitations two electron lenses were installed and are under commissioning. One lens uses a newly manufactured superconducting solenoid, in the other lens the spare superconducting solenoid of the BNL Electron Beam Ion Source (EBIS) is installed to allow for propagation of the electron beam. (This spare magnet will be replaced by the same type of superconducting magnet that is also used in the other lens during the 2013 shut-down.) We give an overview of the commissioning configuration of both lenses, and report on first results in commissioning the hardware. We also report on lattice modifications needed to adjust the phase advance between the beam-beam interactions and the electron lenses, as well as upgrades to the RHIC instrumentation for the commissioning.

INTRODUCTION

In RHIC there are 2 head-on (Interaction Points IP6 and IP8) and 4 long-range (IP2, IP4, IP10, IP12) beam-beam interactions with large separation (10 mm) between beams. The polarized proton luminosity is limited by the head-on effect, and head-on beam-beam compensation is implemented with one electron lens in each ring to compensate for 1 of the 2 head-on collisions. Together with an increase in the bunch intensity an increase in the luminosity by a factor of 2 is anticipated.

The design and construction progress of the RHIC electron lenses was reported previously [1–18], and the main parameters for the proton and electron beams are shown in Table 1. Here we describe the installation after the 2012 summer shut-down, and the progress in commissioning the proton ring lattice and instrumentation, as well as the electron lens hardware.

PROTON BEAM LATTICE AND INSTRUMENTATION

A new lattice was commissioned for both rings that has a phase advance of a multiple of π between IP8 and the electron lens in Interaction Region IR10. This is necessary to minimize resonance driving terms [16]. For this new phase shifter power supplies were installed in both rings

Table 1: Reference cases for RHIC beam-beam and beam-lens interactions. Bunch intensities without electron lenses are expected to saturate at about 2×10^{11} due to head-on beam-beam effects [16].

quantity	unit	value		
proton beam parameters				
total energy E_p	GeV	100	255	255
bunch intensity N_p	10^{11}	2.5	2.5	3.0
$\beta^*_{x,y}$ at IP6, IP8 (p-p)	m	0.85	0.5	0.5
$\beta^*_{x,y}$ at IP10 (p-e)	m	10.0	10.0	10.0
rms emittance ϵ_n, initial	mm mrad		— 2.5 —	
rms beam size at IP6, IP8 σ^*_p	μm	140	70	70
rms beam size at IP10 σ^*_p	μm	485	310	310
rms bunch length σ_s	m	0.50	0.40	0.20
hourglass factor F, initial	...	0.88	0.85	0.93
beam-beam parameter ξ/IP	...	0.012	0.012	0.015
number of beam-beam IPs	...		— 2+1* —	
electron lens parameters				
distance of center from IP	m		— 2.0 —	
effective length L_e	m		— 2.1 —	
kinetic energy E_e	keV	7.8	7.8	9.3
current I_e	A	0.85	0.85	1.10

*One head-on collision in IP6 and IP8 each, and a compensating head-on collision in IP10.

and both transverse planes. In the Blue rings the integer tunes had to be changed from $(28, 29)$ to $(27, 29)$, and in the Yellow ring from $(28, 29)$ to $(29, 30)$ in order to find a solution. With the new lattice higher luminosities were reached than in the previous years, but the polarization was lower. The lower polarization is still under study and may not have been the result of the new lattices. Other lattice options are also under study: (i) A solution was found for the Yellow ring that maintains the integer tunes of $(28, 29)$ and has the correct phase advances; (ii) The phase advance of a multiple of π may also be realized between IP6 and the electron lenses.

A bunch-by-bunch beam loss monitor, based on gated PIN diodes at the primary collimators, was made operational. Figure 1 shows the measured rates for all 109 bunches, and bunches with only 1 collision can be clearly distinguished as having lower loss rates. For the commissioning of the electron lens, a pulsed electron beam that affects only the last proton bunch of the train is available, and the bunch-by-bunch loss monitor can detect the losses of this bunch relative to the others. Transverse BTF measurements are routinely used to monitor the tune, and an algorithm is developed to extract the beam-beam induced tune spread in the presence of coherent modes [20]. A new mode was tested to measure the single bunch response by

* Work supported by Brookhaven Science Associates, LLC under Contract No. DE-AC02-98CH10886 with the U.S. Department of Energy.
† Wolfram.Fischer@bnl.gov

gating the detector.

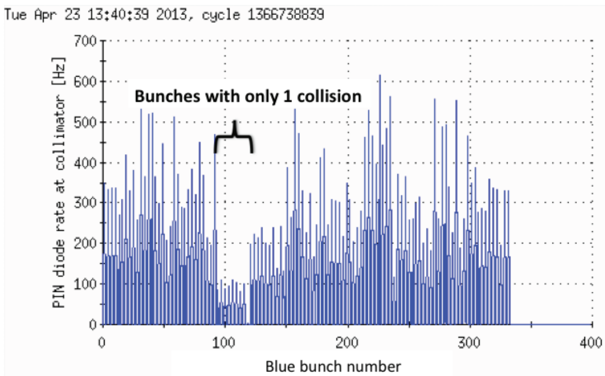

Figure 1: Bunch-by-bunch loss monitor showing lower loss rates for bunches with only 1 collision.

CURRENT LENS INSTALLATION

For the ongoing RHIC Run-13 the hardware of both lenses is partially installed (Fig. 2). The Blue lens has a complete electron beam transport system, although instead of the superconducting main solenoid designed for the electron lens a spare solenoid of the BNL EBIS [19] is installed. This magnet is a 2 m long superconducting solenoid with a maximum field strength of 5 T, but without an iron yoke and therefore field lines that are not straight enough for beam-beam compensation. It does, however, allow for propagation of the electrons from the gun to the collector even at a field as low as 1 T. The low field is necessary in order to minimize the effect on the proton spin as long as the second superconducting solenoid is not yet powered. The Blue lens also has a full complement of instrumentation with the exception of the overlap monitor based on back-scattered electrons [11]. In this configuration all warm magnets can be commissioned as well as the electron beam in pulsed mode. The two dual plane BPMs inside the superconducting solenoid, the YAG screen profile monitor and pinhole detector can be tested. Interaction with the proton beam is possible.

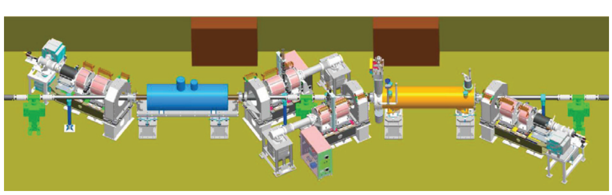

Figure 2: Layout of the two electron lenses in IR10. In 2013 the Blue lens (left) has the EBIS spare solenoid installed instead of the superconducting solenoid designed for the electron lens. In each lens three beams are present, the two proton beams and the electron beam acting on one of the proton beams. The proton beams are vertically separated.

The Yellow lens (Fig. 3) has one of the new superconducting solenoids (designed and manufactured by the BNL Superconducting Magnet Division [10]) installed, but with a straight beam pipe without BPMs or drift tubes (i.e. the vacuum system of the electron gun and collector is not connected to the proton beam vacuum system). This configuration allows for commissioning of the superconducting main solenoid and all superconducting correctors, as well as all warm magnets. Since the superconducting solenoid had been tested only vertically, the installation of the EBIS spare solenoid in the Blue lens guarantees that the electron beam commissioning is not delayed by possible problems with the first horizontal operation of the magnet.

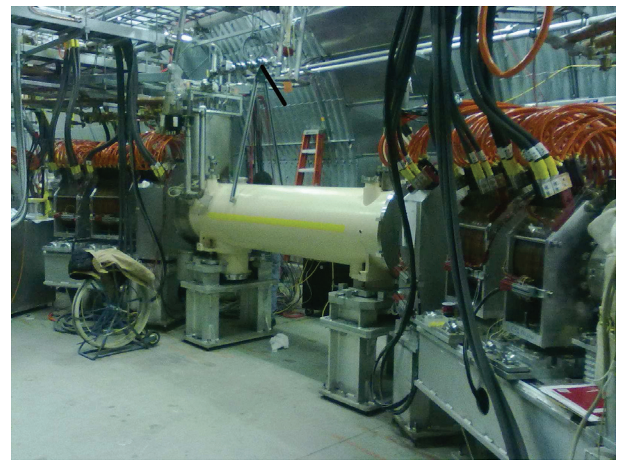

Figure 3: Yellow electron lens as installed in 2013. Visible are the gun side (left), the superconducting main solenoid (center), and the collector side (right).

MAGNET COMMISSIONING

All warm solenoids were tested and ran at operating currents. Their effect on the proton beam [3, 4] was test, and the introduced orbit, tune, and coupling changes were well compensated without any increase in the experimental backgrounds. The warm solenoids will be ramped up to operating current at store, and ramped down when the proton beams are not colliding to save energy (both lenses together consume 0.5 MW of electric power). This is currently being implemented for operation.

Both superconducting solenoids have reached 110% of the 6 T operating field in a vertical test, and are now fully cryostated. The first magnet is installed in the Yellow lens, and final cryo and electrical connections are being made during maintenance periods. Cool-down is expected within a month. The second magnet is set up in the BNL Superconducting Magnet Division to commission a system for the measurement and correction of the field straightness (Fig. 4). With a rms beam size of 310 μm in the electron lenses (Table 1), a straightness tolerance of ± 50 μm was specified over a field range of 1-6 T. The measurement is based on a magnetic needle-and-mirror suspended with a gimbal and calibrated with a vibrating wire [21]. Correction of the field straightness is possible with 5 horizontal and 5 vertical superconducting dipole correctors installed inside of the cryostat [10]. After commissioning of the sys-

ISBN 978-3-95450-122-9

tem, it will be used in the RHIC tunnel to measure and correct the field straightness in-situ.

Figure 4: Test setup for the solenoid field straightness measurement in the BNL Superconducting Magnet Division using one of the two superconducting electron lens solenoids.

INSTRUMENTATION AND SOFTWARE

The Blue lens has new dual plane beam position monitors (BPMs) installed at each end, both of which have been fully commissioned with proton beams and are now part of the RHIC operational orbit control system. The BPMs can be used to stabilize the proton beam orbit in the lens with the orbit feedback [22].

The installation of the Blue gun and collector is also progressing during maintenance periods, and electron beam commissioning is expected to begin before the end of the RHIC Run-13 in June. Due to the slower rise time of the electron beam in pulsed mode, the electron beam signal in the BPMs will be smaller by about an order of magnitude compared to the proton beam. The BPMs will allow for only an approximate positioning of the proton and electron beams. Maximum overlap will be monitored with a backscattered electron monitor [11], which will be installed in the 2013 summer shut-down. With the available electron beam, the electron beam profile monitors (YAG screen and pinhole detector) can also be tested.

The electron lens test stand [14, 18] was already used to develop software for control, measurement analysis, and machine protection. Most of the required functionality is now available for the electron lenses. High level control of the most important parameters is provided through a synoptic display application (Fig. 5), which controls magnetic field strength, electron beam mode (DC or pulsed) and current, and has information on beam position, local losses, and instrumentation devices.

SUMMARY

The main components of the RHIC electron lenses are complete. For 2013 both lenses were partially installed and hardware commissioning is under way. New lattices with

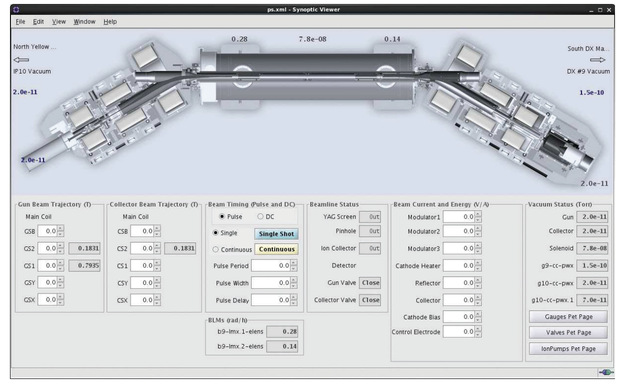

Figure 5: Synoptic display of the electron lens with all high-level data and control points.

the correct phase advance between one of the two beam-beam interactions and the electron lenses were tested in both the Blue and Yellow ring. A high-sensitivity bunch-by-bunch loss monitor was commissioned, and a bunch-by-bunch BTF measurement was tested. The e-lens BPMs of one lens are operational. Control software and the machine protection system were deployed.

In the summer of 2013 the installation of both lenses will be completed. The straightness of the main solenoid field lines will be measured and corrected in-situ. Electron beam commissioning will follow in the subsequent RHIC run.

ACKNOWLEDGMENTS

We are thankful to V. Shiltsev, A. Valishev, and G. Stancari, FNAL, who generously shared their experience with the Tevatron electron lenses. We are grateful to all groups of the BNL Collider-Accelerator Department for their support in the design, construction, and installation of the RHIC electron lenses.

REFERENCES

[1] Y. Luo et al., EPAC'08, pp. 1616.
[2] W. Fischer et al., IPAC'10, pp. 513.
[3] Y. Luo et al., BNL C-AD/AP395 (2010).
[4] X. Gu et al., BNL C-AD/AP/424 (2011).
[5] X. Gu et al., NIM A 637, pp. 190 (2011).
[6] W. Fischer et al., PAC'11, pp. 2223.
[7] A.I. Pikin et al., PAC'11, pp. 2309.
[8] X. Gu et al., PAC'11, pp. 1202.
[9] X. Gu et al., PAC'11, pp. 1205.
[10] R.C. Gupta et al., PAC'11, pp. 1130.
[11] P. Thieberger et al., BIW12, MOPG025.
[12] T.A. Miller et al., BIW12, TUPG039.
[13] W. Fischer et al., IPAC'12, pp. 2125.
[14] X. Gu et al., IPAC'12, pp. 2720.
[15] X. Gu et al., IPAC'12, pp. 4038.
[16] Y. Luo et al., PRSTAB 15, 051004 (2012).
[17] S.M. White et al., IPAC'12, pp. 187.
[18] T.A. Miller et al., IBIC'12, THCB01.
[19] J.G. Alessi et al., LINAC'10, pp. 1033.
[20] P. Görgen et al., Beam-Beam 2013.
[21] A. Jain, presentation at 17^{th} International Magnetic Measurement Workshop, IMMW17, Barcelona, Spain (2011).
[22] M. Minty et al., PAC'11, pp. 1394.